



Sources and depositional pathways of mid-Holocene sediments in the Great Rann of Kachchh, India: Implications for fluvial scenario during the Harappan Culture



Anirban Chatterjee^{a, b, *}, Jyotiranjan S. Ray^a

^a Physical Research Laboratory, Navrangpura, Ahmedabad, 380009, India

^b Department of Geology, The Maharaja Sayajirao University of Baroda, Vadodra, 390002, India

ARTICLE INFO

Article history:

Received 20 February 2017

Received in revised form

29 May 2017

Accepted 3 June 2017

Available online 17 June 2017

Keywords:

Great Rann of Kachchh

Ghaggar-Hakra-Nara river channel

Harappan civilization

Sediments

Geochemistry

ABSTRACT

The decline of the Harappan Culture (5300–3300 yrs BP), one of the earliest urban settlements, has often been linked to the demise of a perennial river (vedic Saraswati?) that originated in the Himalayan Mountain Belt and flowed through the Thar Desert into the Arabian Sea. To test this hypothesis we have studied the mid-Holocene (5.5–1.0 ka) sedimentation history of the Great Rann of Kachchh, an uplifted former gulf of the Arabian Sea, which is believed to have housed the delta of the river. Using trace element geochemistry and Sr-Nd isotopic ratios of sediments as tracers we have determined their provenances. Results of our study suggest that the basin received significant sediment contributions (20–30%) from a distinct sub-Himalayan source, apart from the other proximal sources such as the river Indus, Thar Desert and the ephemeral river Luni. It, however, did not receive any sediment from an independent glacier-fed river. Based on geological and geochemical arguments we infer that these sub-Himalayan sediments could have only been transported through a continuous Ghaggar-Hakra-Nara river channel, possibly seasonal, that flowed through the Harappan heartland. The fact that there was no major change in fluvial sedimentation in the Great Rann of Kachchh and it persisted at least until ~1.0 ka, suggests that drying up of this river system may not have been the primary cause for the decline of the civilization.

© 2017 Elsevier Ltd and INQUA. All rights reserved.

1. Introduction

The Bronze Age Harappan culture is one of the earliest known urban civilizations. Yet, its mysterious decline, within a few centuries of its zenith (4600–3900 yrs BP; Kenoyer, 2008; Possehl, 2002), remains one of the most enigmatic topics in the history of ancient India. The Harappan sites are mostly concentrated along the river systems of Indus and present-day ephemeral Ghaggar-Hakra (which disappears in the Cholistan Desert of Pakistan) and Nara river channel (Fig. 1A). This led to the suggestion that the Ghaggar-Hakra and Nara perhaps was a continuous and perennial fluvial system during the mature Harappan period and that the decline of the civilization was triggered by drying up of the river (Misra, 1984; Mughal, 1997; Wright et al., 2008). Indeed some

workers, with the help of satellite based studies, historical documents and geophysical studies, have identified paleo-river channels that flowed through the present-day arid western margin of Thar Desert into the Arabian Sea (Ghose et al., 1979; Gupta et al., 2011; Sinha et al., 2013; Syvitski et al., 2013) and created a delta system in the western Great Rann of Kachchh (Malik et al., 1999). Moreover, a continuous Ghaggar-Hakra-Nara river system has often been equated with the mythical glacier-fed perennial river Saraswati (Ghose et al., 1979; Kochar, 2000; Oldham, 1893; Pal et al., 1980; Radhakrishnan and Merh, 1999; Valdiya, 2013). Although the presence of buried paleo-channels and a delta complex may hint at the past existence of a fluvial system, in the absence of robust sedimentological and chronological constrains, its existence during the Harappan civilization remains, at the best, a conjecture. Interestingly, sediment provenance studies based on U-Pb dating of detrital zircons along the relict course of Ghaggar-Hakra channel, in its middle segment, seem to suggest that there possibly was a large, glacier-fed Himalayan river along these channels but it was active much before the Harappan civilization in the region, more than 10

* Corresponding author. Physical Research Laboratory, Navrangpura, Ahmedabad, 380009, India.

E-mail address: anirban@prl.res.in (A. Chatterjee).

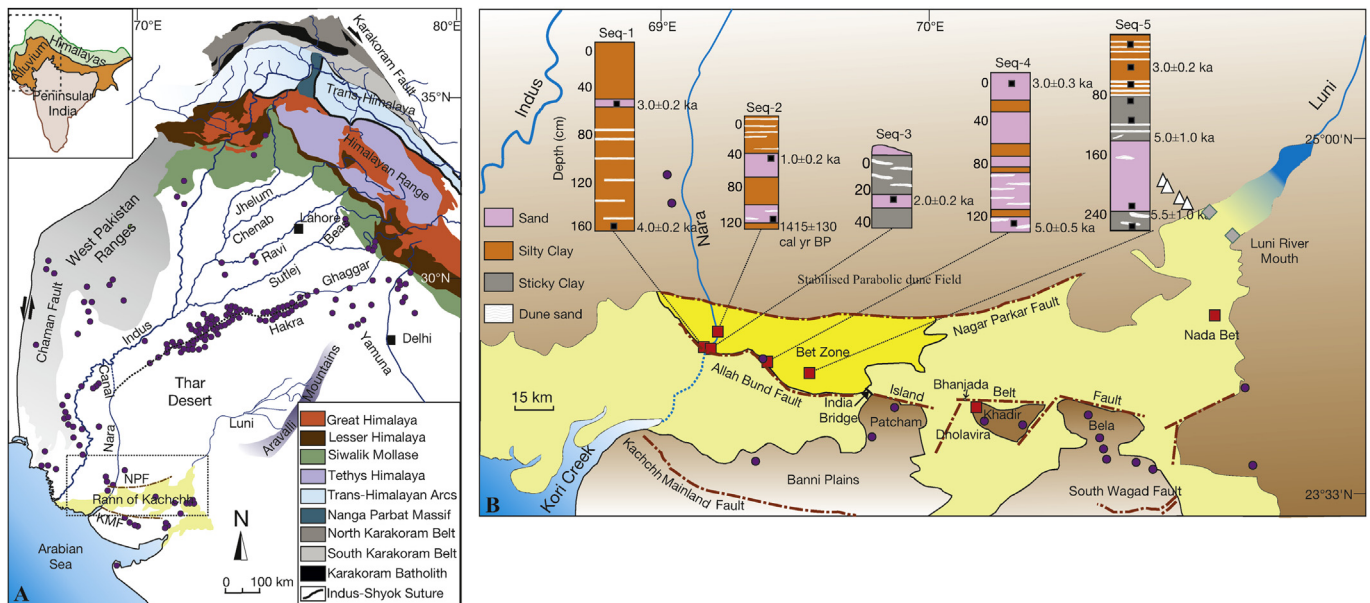


Fig. 1. (A) Schematic geological sketch map (modified from Garzanti et al., 2005) showing the major river systems of north-western India and eastern Pakistan (highlighted portion of the map shown in the inset) and lithology of their catchments. Also shown are different geomorphic features/divisions of the region. The dotted line is the speculated major paleochannel (Vedic Saraswati) that connected the Ghaggar with Hakra and Nara during the Harappan period. NPF = Nagar Parker Fault; KMF = Kachchh Mainland Fault. Harappan sites are marked as purple circles. (B) Schematic sketch map (modified from Tyagi et al., 2012) of the blow up of the area marked in (A) showing the major geological/morphological features of the Great Rann of Kachchh (light/dark yellow) and adjoining region. Sampling locations are marked: red squares for Rann (low lands) and bet (uplifted surfaces), grey diamonds for the Luni river mouth, and white triangles for the Thar dune field. Also shown is the stratigraphy of the sedimentary sequences of the sampled horizons (Seq-1 through Seq-5) in the western Great Rann of Kachchh with OSL/radiocarbon ages marked (in ka/cal yr BP). Positions of the samples on the stratigraphic columns are marked as black squares. (For interpretation of the references to colour in this figure legend, the reader is referred to the web version of this article.)

kyr ago (Clift et al., 2012). These studies also propose that the channels were seasonal (monsoon-fed) during the Holocene (Giosan et al., 2012) and got abandoned during 4–5 ka, eventually getting buried under the parabolic dunes of the Thar Desert by ~1.4 ka (Clift et al., 2012). However, younger fluvial activities (2.9–0.7 ka) have also been reported both from the upper and lower Ghaggar-Hakra floodplains (Giosan et al., 2012). A meandering river system frequently changes its course and creates numerous abandoned channels and therefore, depositional ages of sand from only a few sections may not reveal the true temporal extent of the river (Valdiya, 2013). Furthermore, geochemical studies of Alizai et al. (2011b, 2016) on K-feldspars and garnets in sediments of the river Nara suggest that either Nara was a former distributary of the river Indus or it was an ephemeral stream receiving reworked sediments. However, the former idea seems less likely as Tyagi et al. (2012) have clearly demonstrated that no major river system had flowed into the Nara channel since mid-Holocene.

In the above scenario, the Great Rann of Kachchh (GRK) of western India (Fig. 1A), which is located in the confluence zone between the lost river (vedic Saraswati?) and the Arabian Sea (Valdiya, 2013), becomes an important piece of the puzzle. Located marginally above the mean sea level (~4 m), the GRK is a desolate landscape of salty wasteland. It is believed to have supported maritime activities of the Harappans (Gaur et al., 2013) as evident from the ruins of Dholavira, one of the major Harappan towns - located in the very heart of the GRK, and many such sites in the region (Fig. 1B). While the eastern GRK primarily receives fluvial contribution from the river Luni, the western GRK is inundated by storm tides during the southwest Indian monsoon (Glennie and Evans, 1976), and receives some contribution from the ephemeral Nara during flooding in the Indus (Fig. 1A), channelized through man-made canals (Syvitski et al., 2013). Sediments exposed in structurally raised sandy mounds ('bet' in local language) and layered sand-silt sediments in the terraces around the margins of

the islands (Patcham, Khadir and Bhanjada; Fig. 1B) bear testimony to a fluvial past of the GRK. Therefore, unravelling of the sedimentation history of the GRK since the mid-Holocene, besides being geologically important, has profound geo-archaeological implications towards deciphering the existence of any notable fluvial system (other than Indus) during the proliferation of Harappan civilization. To investigate this aspect of the GRK, we have studied trace element and Sr-Nd isotope geochemistry of sediments deposited in the basin during the last 5.5 kyr (Fig. 1), and quantified, for the first time, sediment contributions from various terrigenous sources. We have also made an attempt to decipher sediment transport pathways in order to throw light on the fluvial scenario of the Harappan period and in the process explored possible existence of a glacial fed river, originating from the higher Himalaya, draining into the Kachchh basin. Our samples came from the relict delta of the river Nara – the purported delta of the Saraswati, central and eastern GRK, mouth of the river Luni, and dunes of the southern-eastern Thar Desert (Fig. 1B).

2. Study area and sampling

2.1. The Great Rann of Kachchh

The GRK is an enigmatic geomorphic terrain that encompasses a vast stretch of low-lying salty desert (~16,000 sq. km) at the western margin of India, and is devoid of any major drainage; except for the ephemeral river Luni and river Nara (Fig. 1). It is flanked by parabolic dunes in the north and northwest, Banni Plain and the Wagad Upland in the south (Fig. 1B). Structurally, the GRK is part of an east-west trending paleo-rift graben believed to have formed in the Early Mesozoic (Biswas, 1987) and is bounded in the north by the Nagar Parkar Fault and in the south by the Kachchh Mainland and the South Wagad faults (Fig. 1B). In between, there exist two other east-west trending faults; namely the Allah Bund

and Island Belt (Fig. 1B), which are known to have influenced the Quaternary morphology of the GRK (Mathew et al., 2006; Maurya et al., 2008; Rajendran and Ranjendran, 2001). It has been suggested that the present day Rann surface is an uplifted floor of a former shallow marine gulf of the Arabian Sea that had formed during sea level rise at the immediate aftermath of the last glacial period (Maurya et al., 2008; Merh, 2005; Oldham, 1926). The latest uplift is believed to have occurred at ~2 kyr ago (Tyagi et al., 2012). At present, the central and eastern GRK remains detached from the western GRK, along a median high that passes through north-west of the Patcham Island along the India Bridge (Fig. 1B).

Monotonously flat topography, except for small bays, makes it difficult to determine the history of sedimentation in the GRK. It is believed that much of the Holocene sediments in the western part of the basin were derived from the Indus and Nara rivers that once flowed into the basin (Glennie and Evans, 1976; Khonde et al., 2016). Modern silty-clay deposits are attributed to storm tides, which bring in material from the Indus Delta aided by long-shore current, during the southwest monsoon (Glennie and Evans, 1976; Tyagi et al., 2012). The Banni Plain, which receives sediments from the Mesozoic sedimentary rocks of the northern Kachchh Mainland (Glennie and Evans, 1976; Maurya et al., 2013; Fig. 1B), acts as a buffer between the Mainland and the western GRK. Considering that the dry highlands and deserts surround the entire GRK, it is reasonable to expect aeolian contribution in the Rann sedimentation during periods of intense wind activity.

2.2. Sampling strategy and samples

Sediment samples for the present study were collected from tectonically raised surfaces or terraces, incised channels and dug up trenches (Fig. 1B). Since the primary focus of the study was the purported delta of the mythical river, we planned to examine in detail the bay zone north of the Allah Bund Fault scarp (Fig. 1B). Samples from this zone came from five sequences in five locations, in the western GRK, which were topographically higher than the present-day high tide strands. Fig. 1B presents stratigraphy of these horizons and the already known depositional ages from the work of Tyagi et al. (2012). Three of the sampling locations were on or near the channel of the river Nara (Fig. 1B). Samples representing the central and eastern GRK were collected from the western periphery of Khadir Island and from Nada Bay (Fig. 1B). These samples are sub-recent sediments exposed on fault controlled terraces, which occur as sandy deposits in the centre of silt dominated GRK basin. The geomorphology of these sites suggests that these sediments were derived from the surrounding rocky islands containing Mesozoic sediments and transported by local drainage. Apart from the river Nara, other potential sources of sediments to the western GRK during the mid-Holocene include the Thar Desert, the river Luni, and the river Indus.

The Thar Desert occurs as the most dominant landscape along the northern margin of the GRK basin. In absence of any fluvial system from the desert into the Great Rann of Kachchh basin, the only mode of sediment transportation from the northern margin could have been through wind. There was a need to characterize this source as only limited geochemical data existed that to from the far north-eastern margin of the desert, located ~800 km inland (Tripathi et al., 2013). In any case, the dune field at this margin cannot be considered as a potential aeolian sediment source for the GRK since the southwest monsoonal winds are believed to be the primary carrier of the desert sand (Singhvi and Kar, 2004). However, aeolian contribution from the sand dunes present in the near vicinity of the GRK is more likely through local sand storms and disturbances as they lack directionality. Therefore, to accurately

predict sediment contribution from the Thar, we planned to sample sand dunes that are located very close to the northern margin of the GRK. However, because of inaccessibility of the north-western and northern margin of the basin (located in Pakistan), we could sample only the dunes located along the north-eastern margin (Fig. 1B). These samples were sub-recent sediments from stabilized parabolic dune field.

Luni is the only river system in India that drains from the Aravalli mountain ranges into the GRK (Fig. 1). The river remains ephemeral since ~8 ka (Kar et al., 2001), therefore, the sediment supply through it takes place only during heavy rainfall events linked to the southwest Indian monsoon. Because of its very nature, sediments transported by the Luni are mostly consisting of reworked alluvial and aeolian deposits. To constrain its contribution to the GRK we sampled sub-surface sediments along the river mouth (Fig. 1B). These samples would likely to provide average compositions of the Holocene sediments transported by the river.

Although the river Nara today brings in sediments from the river Indus into the GRK, there exists no evidence to suggest if the same was true in the past. However, it has been recognized that recycled Indus sediments have been getting into the basin through creeks via tidal currents as suspended load (mostly clay, Tyagi et al., 2012). In this work we make use of the geochemical data of Clift et al. (2010) and Limmer et al. (2012) for such sediments.

3. Methods

Nine sediment samples were dated by OSL method using single aliquot regeneration (SAR) protocol of (Murray and Wintle, 2000), whereas one sample of gastropod shells was dated by radiocarbon method using conventional β -counting (Yadava and Ramesh, 1999). Texturally, the samples are dominated by fine-grained sand and silty-clay which were believed to have been deposited in a tidal flat environment (Tyagi et al., 2012). As per the age information, the sediment samples from the western GRK, studied for geochemistry, represent a depositional history between 5.5 and ~1.0 kyr BP.

All the geochemical and isotopic measurements were done on silicate fractions of bulk sediments. Samples were washed with MILLI-Q water multiple times to remove salt, dried at 110 °C, powdered and homogenised. Prior to dissolution, powdered samples were heated at 650 °C for 2 h to remove organic matter and leached in dilute HCl to remove carbonates. Decarbonated samples were then dissolved using standard HF-HNO₃-HCl dissolution procedure for silicates. Concentrations of trace elements including rare earth elements (REEs) were measured using a Q-ICPMS at Physical Research Laboratory (PRL). USGS rock standard BHVO-2 was used as unknown for accuracy check. Reproducibility of trace element contents, based on repeated analyses of the standard, was $\leq 3\%$ for REEs and $\leq 6\%$ for all other trace elements at 2σ level. Sr separation was done by conventional cation exchange column chemistry and Nd was separated from other REEs using Ln-specific resin from Eichrom with dilute HCl as elutant. $^{87}\text{Sr}/^{86}\text{Sr}$ and $^{143}\text{Nd}/^{144}\text{Nd}$ were measured in static multicollection mode on an Isoprobe-T TIMS (Awasthi et al., 2014). The measured isotopic ratios were corrected for fractionation using $^{86}\text{Sr}/^{88}\text{Sr} = 0.1194$ and $^{146}\text{Nd}/^{144}\text{Nd} = 0.7219$, respectively. The average values for NBS987 and JNdi measured over a period of 5 years are $^{87}\text{Sr}/^{86}\text{Sr} = 0.71023 \pm 0.00001$ ($n = 70$) and $^{143}\text{Nd}/^{144}\text{Nd} = 0.512104 \pm 0.000004$ ($n = 60$; ± 0.1 in ϵ_{Nd} units) at 2σ level of uncertainty. The value of $^{143}\text{Nd}/^{144}\text{Nd} = 0.512104$ for JNdi corresponds to a value of 0.511847 for the widely used La Jolla Nd standard (Tanaka et al., 2000). $^{87}\text{Sr}/^{86}\text{Sr}$ and $^{143}\text{Nd}/^{144}\text{Nd}$ for BHVO-2 measured gave values of 0.70346 ± 0.00004 and 0.512967 ± 0.000008 ($n = 10$; ± 0.2 in ϵ_{Nd} units at 2σ) respectively, which are same as the reported values of 0.70344 ± 0.00003 and

0.51296 ± 0.00004 within 2σ (Raczek et al., 2001). To compare our data with that from literature, all the $^{87}\text{Sr}/^{86}\text{Sr}$ and $^{143}\text{Nd}/^{144}\text{Nd}$ ratios were normalized to 0.71025 for NBS987 and 0.511858 for La Jolla, respectively. All plots and discussion below are based on the normalized ratios.

4. Results and discussion

4.1. Geochemistry of siliciclastic sediments

Our geochemical and isotopic data for bulk sediment samples and different grain size fractions from them are presented in Tables 1 and 2, respectively. The chondrite normalized REE patterns for the GRK sediments show pronounced light REE (LREE) enrichment and a negative Eu anomaly (not presented here) - characteristics of continental crust derived detritus. The upper continental crust normalized patterns show a flat LREE and depleted heavy REE (HREE) pattern (not presented here), with the latter possibly hinting at removal of heavy minerals such as zircon from sediments prior to their deposition in the basin. Negative anomalies of Zr and Hf and depleted patterns of HREE seen in the Post Archean Australian Shale (PAAS) normalized trace element data for these samples (Fig. 2A) are consistent with the above observation. Interestingly, these patterns are, to a large extent, comparable to that observed in the sediments in the five major rivers of Punjab (Alizai et al., 2011a) and sand dunes of the Thar, however, are different from that reported for the sediments from the Indus Delta (Clift et al., 2002, Fig. 2A). This is at variance with the earlier belief that the western GRK is predominantly filled with the Indus derived sediments (Maurya et al., 2003; Tyagi et al., 2012). To further understand the nature of probable sediment sources we have made use of various cross plots of elemental and isotopic ratios wherein the fields of these sources (end-members) could be easily distinguished (Fig. 2B–D). Sediments from the Indus is known to enter the western GRK through the Kori Creek with the help of long-shore currents, and having significant contributions from the juvenile (mantle derived) rocks of the Indus-Tsangpo Suture Zone (ITSZ). These have higher Nb/Ba, Cr/Th, ϵ_{Nd} and Sr content, and lower $^{87}\text{Sr}/^{86}\text{Sr}$ and Th/Y compared to the Higher-Himalaya-derived sediments in the five rivers of Punjab. Absence of adequate geochemical data does not allow us to create a field/envelope for the Thar Desert; however, we make use of our data from the dune field at the north-eastern margin of the GRK for comparisons. In these plots most of our samples fall in the space in-between the two major end-members (Fig. 2B–D) suggesting contributions from all of these sources, not just the Indus, to the sediment budget of the GRK.

Being rare-earth elements, the Sm-Nd system is not easily disturbed by the surficial processes like erosion, transportation and sedimentation (Goldstein and Jacobsen, 1988; Najman, 2006). Hence, this systematics is ideal for bulk sediment provenance study. The measured ϵ_{Nd} of samples (with a precision of ±0.2 at 2σ) from the western GRK, the southern Thar Desert and the Luni river mouth varies in ranges of −14.3 to −11.4, −11.8 to −11.0, and −12.5 to −11.5, respectively. In Fig. 3, we compare these data with that from the Holocene sediments in the Ghaggar-Hakra channels, Indus delta and Indus shelf (Alizai et al., 2011a; Clift et al., 2008; East et al., 2015; Limmer et al., 2012; Singh et al., 2016a). From Fig. 3 it can be inferred that since mid-Holocene there has been little influence of Sutlej or Yamuna in western GRK sedimentation excluding the possibilities of the sediments being transported by Greater Himalayan glacier-fed rivers. On the contrary, ϵ_{Nd} of the GRK sediments overlap with that observed in the north-eastern Thar Desert, deposited during 9.1 to 1.8 ka (Fig. 3A). However, as discussed in the previous section, the only possible mode by which this distal source

Table 1
Geochemical data for sediment samples from the Great Rann of Kachchh.

Sample	SBTL-1 ^K	NRMOSL-1 ^K	ABP-1a ^K	KHTL-1 ^D	KSTL-1 ^K
Cs	1.92	3.84	3.99	8.33	3.97
Rb	64.2	94.4	91.8	123.1	90.4
Ba	313	363	354	402	348
Th	13.5	12.3	16.1	8.1	10.4
U	1.83	1.64	2.07	1.50	1.42
Nb	8	11	11	14	10
Ta	1.77	0.85	0.91	0.93	1.62
La	37	35	43	19	28
Ce	77	72	86	39	58
Pb	12.2	13.1	15.3	8.4	12.8
Pr	9.4	8.5	10.2	4.7	7.1
Sr	128	134	129	79	117
Nd	31	27	33	16	23
Zr	12	13	15	49	11
Hf	0.4	0.4	0.5	1.5	0.4
Sm	6.3	5.7	6.7	3.2	4.8
Eu	1.2	1.1	1.2	0.7	1.0
Gd	5.5	4.9	5.9	2.8	4.1
Tb	0.60	0.53	0.63	0.32	0.46
Dy	3.5	3.1	3.7	2.1	2.7
Y	13.6	12.1	14.6	9.1	10.7
Ho	0.58	0.50	0.61	0.38	0.46
Er	1.6	1.5	1.8	1.2	1.3
Tm	0.2	0.2	0.2	0.2	0.2
Yb	1.2	1.1	1.3	1.0	1.0
Lu	0.16	0.15	0.18	0.15	0.13
Sc	6.7	7.3	8.4	11.0	6.7
V	39	49	56	86	43
Cr	23	33	38	67	29
Co	3	4	5	7	4
$^{87}\text{Sr}/^{86}\text{Sr}$	0.72878	0.72853	0.72743	0.71553	0.72982
$^{143}\text{Nd}/^{144}\text{Nd}$	0.511907	0.511930	0.511906	0.511982	0.511935
$\epsilon_{\text{Nd}}(0)$	−14.3	−13.8	−14.3	−12.7	−13.7
Sample	KHTL-3 ^D	BBMF ^K	KH/DV/TL1 ^D	ABP-2 ^K	KSTL-2 ^K
Cs	1.48	9.28	3.88	7.57	7.75
Rb	46.2	160.1	73.6	131.9	137.3
Ba	281	497	17	427	426
Th	5.4	10.4	4.8	10.3	9.7
U	0.80	1.36	0.79	1.37	1.33
Nb	5	12	6	7	7
Ta	0.38	0.75	0.38	0.56	0.61
La	15	29	11	29	26
Ce	32	62	26	60	59
Pb	7.4	12.7	3.0	12.2	12.7
Pr	3.8	7.2	3.3	7.2	6.6
Sr	63	109	128	111	112
Nd	12	23	11	23	21
Zr	20	14	18	12	8
Hf	0.6	0.5	0.6	0.4	0.3
Sm	2.5	4.7	2.2	4.8	4.4
Eu	0.5	1.0	0.5	1.0	0.9
Gd	2.0	4.0	1.8	4.1	3.7
Tb	0.21	0.43	0.19	0.43	0.40
Dy	1.3	2.5	1.2	2.5	2.3
Y	5.4	9.2	4.6	9.5	8.7
Ho	0.22	0.40	0.20	0.42	0.38
Er	0.7	1.2	0.6	1.2	1.1
Tm	0.1	0.1	0.1	0.1	0.1
Yb	0.6	0.9	0.5	0.9	0.8
Lu	0.08	0.12	0.07	0.12	0.11
Sc	3.3	12.2	5.6	9.9	9.6
V	33	97	45	77	68
Cr	25	63	32	49	45
Co	2	8	4	7	8
$^{87}\text{Sr}/^{86}\text{Sr}$	0.72327	0.72723	0.71459	0.72896	0.72937
$^{143}\text{Nd}/^{144}\text{Nd}$	0.511915	0.511936	0.511968	0.511927	0.511942
$\epsilon_{\text{Nd}}(0)$	−14.1	−13.7	−13.1	−13.9	−13.6
Sample	KRNOSL-3 ^K	ABTL-2 ^K	SBTL-4 ^K	KH/DV/TL2 ^D	BdB(b)-1 ^K
Cs	0.77	3.79	4.34	5.82	6.60
Rb	39.3	90.4	99.9	99.6	130.6

Table 1 (continued)

Sample	SBTL-1 ^K	NRMOSL-1 ^K	ABP-1a ^K	KHTL-1 ^D	KSTL-1 ^K
Ba	201	375	438	394	420
Th	1.3	11.4	11.8	7.0	7.5
U	0.30	1.89	1.84	1.11	1.23
Nb	3	12	14	8	11
Ta	0.13	1.00	1.05	0.43	0.80
La	3	33	34	20	20
Ce	6	68	70	41	41
Pb	8.4	15.6	11.5	10.0	13.8
Pr	0.7	8.3	8.5	4.9	5.1
Sr	41	121	118	106	114
Nd	2	26	27	15	16
Zr	8	16	20	20	13
Hf	0.3	0.6	0.7	0.7	0.5
Sm	0.5	5.7	5.7	3.1	3.5
Eu	0.2	1.2	1.1	0.7	0.8
Gd	0.5	4.9	4.9	2.6	3.0
Tb	0.06	0.56	0.54	0.27	0.34
Dy	0.4	3.4	3.3	1.6	2.1
Y	1.7	13.0	12.6	5.9	7.9
Ho	0.08	0.58	0.55	0.27	0.36
Er	0.2	1.7	1.6	0.8	1.1
Tm	0.0	0.2	0.2	0.1	0.1
Yb	0.2	1.3	1.2	0.7	0.8
Lu	0.03	0.18	0.16	0.09	0.11
Sc	1.2	8.5	8.9	8.1	8.8
V	14	53	60	64	65
Cr	4	37	40	45	44
Co	1	4	3	5	7
⁸⁷ Sr/ ⁸⁶ Sr	0.72141	0.72800	0.72869	0.72423	0.72961
¹⁴³ Nd/ ¹⁴⁴ Nd	0.512053	0.511947	0.511925	0.511986	0.511971
ε _{Nd} (0)	-11.4	-13.5	-13.9	-12.7	-13.0

Sample	NRMOSL-3 ^K	GdB-2 ^K	C-16/13 ^K	C-16/17 ^K	C-16/21 ^K
Cs	2.81	7.09	4.97	11.98	5.27
Rb	79.3	136.7	111.2	192.3	111.4
Ba	365	445	429	538	419
Th	11.2	6.8	12.1	10.4	12.0
U	1.79	1.02	1.95	1.79	1.87
Nb	10	11	14	20	13
Ta	0.73	0.73	0.96	1.27	0.92
La	33	19	33	25	32
Ce	67	40	70	58	67
Pb	13.7	13.6	12.7	10.2	12.5
Pr	8.2	4.8	8.3	6.1	8.1
Sr	137	112	126	83	117
Nd	26	15	27	20	25
Zr	12	10	20	50	16
Hf	0.4	0.4	0.7	1.4	0.6
Sm	5.7	3.3	5.7	4.0	5.5
Eu	1.2	0.8	1.2	0.8	1.1
Gd	4.9	2.9	4.9	3.5	4.8
Tb	0.56	0.31	0.55	0.39	0.54
Dy	3.5	1.9	3.4	2.4	3.3
Y	13.3	7.0	13.0	10.2	12.2
Ho	0.58	0.32	0.56	0.45	0.56
Er	1.7	0.9	1.7	1.4	1.6
Tm	0.2	0.1	0.2	0.2	0.2
Yb	1.3	0.7	1.3	1.2	1.2
Lu	0.17	0.09	0.17	0.16	0.16
Sc	7.9	8.6	9.5	13.6	9.8
V	49	61	65	119	69
Cr	32	45	43	76	42
Co	3	6	4	7	4
⁸⁷ Sr/ ⁸⁶ Sr	0.72725	0.73066	0.72832	0.73064	0.72881
¹⁴³ Nd/ ¹⁴⁴ Nd	0.511953	0.511952	0.511930	0.511970	0.511978
ε _{Nd} (0)	-13.4	-13.4	-13.8	-13.0	-12.9

Sample	C-16/26 ^K	NB-1 ^N	MS-1 ^L	BKS-4 ^L	BKS-1 ^T
Cs	4.97	0.47	1.46	1.25	1.53
Rb	110.7	23.9	64.6	57.8	55.9
Ba	451	128	340	315	281
Th	12.2	6.0	5.5	8.1	6.7

Table 1 (continued)

Sample	SBTL-1 ^K	NRMOSL-1 ^K	ABP-1a ^K	KHTL-1 ^D	KSTL-1 ^K
U	1.58	1.43	0.79	1.12	0.94
Nb	9	2	4	5	6
Ta	0.61	0.06	0.32	0.91	0.55
La	35	11	15	24	23
Ce	73	21	29	50	45
Pb	11.8	4.0	13.0	12.3	4.7
Pr	8.8	2.4	3.5	6.0	4.9
Sr	118	34	119	123	167
Nd	28	7	11	19	18
Zr	80	14	7	10	13
Hf	2.1	0.5	0.3	0.4	0.4
Sm	5.9	1.4	2.2	3.9	3.1
Eu	1.2	0.3	0.6	0.8	0.7
Gd	4.9	1.2	1.9	3.3	2.9
Tb	0.53	0.14	0.22	0.36	0.34
Dy	3.0	0.9	1.4	2.2	2.0
Y	11.1	3.6	5.6	8.7	9.8
Ho	0.50	0.15	0.23	0.37	0.36
Er	1.4	0.5	0.7	1.1	1.1
Tm	0.2	0.1	0.1	0.1	0.1
Yb	1.0	0.4	0.5	0.9	1.0
Lu	0.14	0.06	0.07	0.12	0.13
Sc	9.6	1.6			5.8
V	65	10			41
Cr	38	6	11	20	58
Co	4	1	2	2	3
⁸⁷ Sr/ ⁸⁶ Sr	0.72837	0.72303	0.72794	0.72610	0.72516
¹⁴³ Nd/ ¹⁴⁴ Nd	0.511933	0.511969	0.511997	0.512050	0.512047
ε _{Nd} (0)	-13.8	-13.1	-12.5	-11.5	-11.5

Sample	BKS-1-CLAY ^T	BKS-2 ^T	BKS-3 ^T	BKS-5 ^T	BHVO-2
Cs	3.60	1.73	1.65	1.08	0.12
Rb	75.0	64.0	57.0	40.3	10.3
Ba	260	313	280	201	130
Th	16.1	6.3	5.0	6.4	1.1
U	3.37	0.72	0.62	0.63	0.42
Nb	13	5	4	3	17
Ta	0.46	0.47	0.30	0.28	0.95
La	32	21	18	21	15
Ce	78	40	36	41	39
Pb	2.7	5.2	5.9	4.1	1.2
Pr	7.3	4.3	4.0	4.4	5.2
Sr	72	168	143	96	388
Nd	23	15	11	11	24
Zr	181	16	7	13	163
Hf	5.8	0.5	0.3	0.5	3.9
Sm	5.0	2.7	2.6	2.5	5.9
Eu	0.9	0.7	0.8	0.6	2.0
Gd	5.1	2.5	2.4	2.4	6.1
Tb	0.67	0.30	0.28	0.27	0.84
Dy	4.6	1.9	1.6	1.5	5.2
Y	22.0	9.2	6.0	5.5	23.4
Ho	0.92	0.34	0.30	0.29	0.89
Er	3.0	1.1	0.9	0.9	2.5
Tm	0.4	0.1	0.1	0.1	0.3
Yb	3.0	1.0	0.8	0.9	1.9
Lu	0.44	0.14	0.11	0.13	0.26
Sc	9.5	6.1	3.9	3.1	31.6
V	78	32	27	22	337
Cr	71	27	14	14	291
Co	3	3	2	2	48
⁸⁷ Sr/ ⁸⁶ Sr	0.71307	0.72648	0.72758	0.72429	0.70346
¹⁴³ Nd/ ¹⁴⁴ Nd	0.512077	0.512031	0.512049	0.512074	0.512967
ε _{Nd} (0)	-11.0	-11.8	-11.5	-11.0	6.4

Superscripts: ^K = Western Great Rann of Kachchh; ^D = Khadir Island, Eastern Great Rann of Kachchh; ^N = Nada Bet, Eastern Great Rann of Kachchh; ^L = Luni River mouth; ^T = Thar dune sand. Trace element concentrations are in ppm. Data for BHVO-2 is averages of 10 analyses. ε_{Nd} = [(¹⁴³Nd/¹⁴⁴Nd)_{sample} / (¹⁴³Nd/¹⁴⁴Nd)_{Chondrite} - 1] × 10⁴. (¹⁴³Nd/¹⁴⁴Nd)_{Chondrite} is taken as 0.512638. External reproducibility (2σ) of ⁸⁷Sr/⁸⁶Sr and ε_{Nd} determined by multiple analyses of NBS987 and JNdi-1 are ±0.000001 and ±0.1, respectively.

Table 2
Isotopic data for different grain sizes separated from sediments of the Nara river mouth and Western Great Rann of Kachchh.

Grain Size	NRM-OSL-1C	NRM-OSL-2C	NRM-OSL-3C	KRM-OSL-1C	KRM-OSL-2C	KRM-OSL-3C
<4 μm						
$^{87}\text{Sr}/^{86}\text{Sr}$	0.72427	0.72438	0.72409	0.72427	0.72079	0.72257
$^{143}\text{Nd}/^{144}\text{Nd}$	0.51198	0.511968	0.512001	0.511984	0.511982	0.512007
$\epsilon_{\text{Nd}}(0)$	-12.8	-13.1	-12.4	-12.8	-12.8	-12.3
4–15.6 μm						
$^{87}\text{Sr}/^{86}\text{Sr}$	0.72568	0.72559	0.72562	0.72570	0.72124	0.7222
$^{143}\text{Nd}/^{144}\text{Nd}$	0.511981	0.511949	0.511946	0.511976	0.512012	0.511963
$\epsilon_{\text{Nd}}(0)$	-12.8	-13.4	-13.5	-12.9	-12.2	-13.2
45–75 μm						
$^{87}\text{Sr}/^{86}\text{Sr}$	0.72741	0.72849	0.72674	0.72999	0.72495	0.72087
$^{143}\text{Nd}/^{144}\text{Nd}$	0.511962	0.511966	0.511956	0.511948	0.511926	0.511957
$\epsilon_{\text{Nd}}(0)$	-13.2	-13.1	-13.3	-13.5	-13.9	-13.3
75–90 μm						
$^{87}\text{Sr}/^{86}\text{Sr}$	0.73140	0.73576	0.73463	0.73138	0.72672	0.72060
$^{143}\text{Nd}/^{144}\text{Nd}$	0.511974	0.511943	0.511963	0.511973	0.512003	0.512064
$\epsilon_{\text{Nd}}(0)$	-12.3	-13.6	-13.2	-13.0	-12.4	-11.2

could have contributed is through reworking by a fluvial system. The present-day ephemeral Ghaggar-Hakra river system, which is believed to have been connected to the Nara during the mid-Holocene (Valdiya, 2013), is the most suitable candidate for the above pathway. The overlapping ϵ_{Nd} values of pre-modern sediments in the Ghaggar-Hakra system with that of the western GRK sediments (Fig. 3B) may be considered as an evidence for the above. It is also observed that ϵ_{Nd} data from GRK sediments overlap with that of the sediments in the Indus delta (Fig. 3B), however, they do not follow the regional trend (with age) shown by the latter thus making it an unlikely source. The trend seen in the GRK data (Fig. 3B) appears to

suggest mixing between sediments from the Ghaggar-Hakra fluvial system (containing reworked aeolian sand from northern desert margin) and Indus borne detritus, in addition to possible contributions from the Luni and the southern Thar (Fig. 3A and B).

4.2. Grain size and isotopic compositions

For a better characterization of the provenances, we utilize Sr isotopic ratios of these sediments along with their Nd isotopic ratios, keeping in mind the limitations of the former (Najman, 2006). It is generally believed that unlike the ^{147}Sm - ^{143}Nd isotopic system,

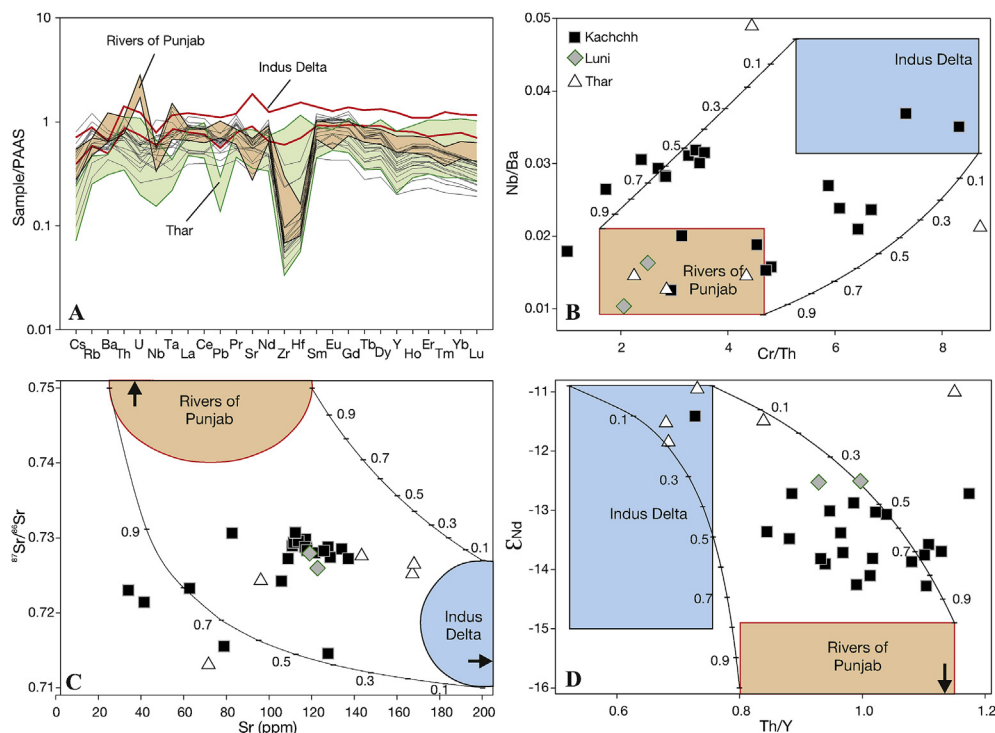


Fig. 2. (A) PAAS normalized multi-element trace element patterns of sediment samples from the Great Rann of Kachchh (this work) compared with that of sediments from rivers of Punjab (Orange field; Alizai et al., 2011a), Indus delta sediments (red envelop; Clift et al., 2002), and Thar desert sand (green field; this work). (B) Nb/Ba vs. Cr/Th (C) $^{87}\text{Sr}/^{86}\text{Sr}$ vs. Sr, and (D) ϵ_{Nd} vs. Th/Y plots for the Kachchh, Luni and Thar samples compared with binary mixing model curves drawn considering sediments in Indus delta and rivers of Punjab as two end-members. Tick marks on mixing curves are fraction of Punjabi rivers' contributions to the mixture. (For interpretation of the references to colour in this figure legend, the reader is referred to the web version of this article.)

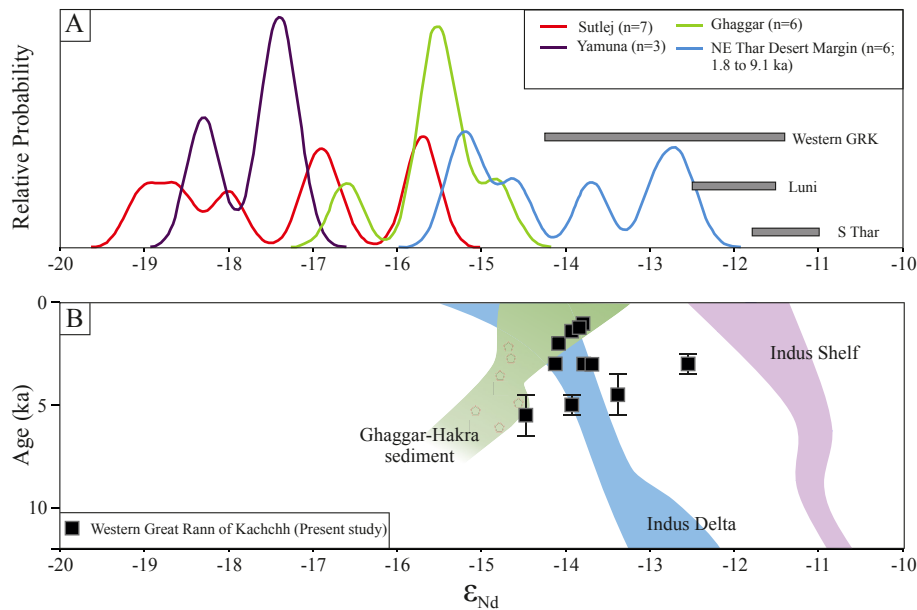


Fig. 3. (A) Kernel density estimation (KDE) plot of ϵ_{Nd} re-drawn from (Singh et al., 2016b) displaying the Nd-isotopic variability in Sutlej, Yamuna, Ghaggar and Thar desert (present work and Singh et al., 2016a; Tripathi et al., 2013). (B) The Western Great Rann of Kachchh sediments deposited since 5.5 ka are compared with the sediments of Ghaggar-Hakra River (East et al., 2015; Singh et al., 2016a), Indus delta (Clift et al., 2010) and shelf (Limmer et al., 2012) deposited during the Holocene.

the ^{87}Rb - ^{87}Sr system is susceptible to chemical weathering which leads to dissimilar Sr isotopic ratio between the source rocks and the product sediments (Meyer et al., 2011). Higher chemical weathering leads to more radiogenic detritus which is largely controlled by higher $^{87}\text{Sr}/^{86}\text{Sr}$ bearing fine-grained (clay) fraction, primarily derived from high-Rb bearing micas in the source rocks (Garçon et al., 2014; Meyer et al., 2011). Below we discuss the effect of grain size on Sr isotopic composition of the GRK sediments and evaluate its bearing on determination of provenances.

Six western GRK samples were selected for studying the effect of grain size on the $^{87}\text{Sr}/^{86}\text{Sr}$ variation. Different grain size fractions were separated namely: clay ($<4\mu$), silt (4–15.6 μ), fine sand (45–75 μ) and coarse sand (75–90 μ). By weight coarse sand was found to be the dominant fraction ($>70\%$) in these samples. All the fractions were decarbonated using dilute HCl before being analyzed for Sr and Nd isotopic compositions. These data are presented in Fig. 4. As can be seen from the data, although there is a large variation of $^{87}\text{Sr}/^{86}\text{Sr}$, it shows an overall increasing trend with increasing grain

size (Fig. 4A). This is entirely opposite of what is generally observed in most fluvial systems where in the finest fractions (suspended load/clay) contain more radiogenic Sr than the coarser fractions (Garçon et al., 2014).

One plausible explanation for the observation could be that different sources with distinct isotopic signature contributed to different grain size fractions. However, such a phenomenon should have been reflected more prominently in Nd isotopic compositions, because ϵ_{Nd} is a more robust provenance indicator compared to $^{87}\text{Sr}/^{86}\text{Sr}$. However, we do not observe any such dependency in Fig. 4B. In fact a closer look reveals that different grain size fractions of four samples possess overlapping ϵ_{Nd} (within ± 0.5 , where experimental reproducibility is ± 0.2 at 2σ). We therefore believe that the observed variation of $^{87}\text{Sr}/^{86}\text{Sr}$ ratios with grain-size (Fig. 4A) is a product of lesser chemical weathering compared to physical weathering in the source, similar to that observed in many parts of the Himalaya (Singh et al., 2008). Since during chemical weathering, high-Rb bearing minerals (containing high radiogenic

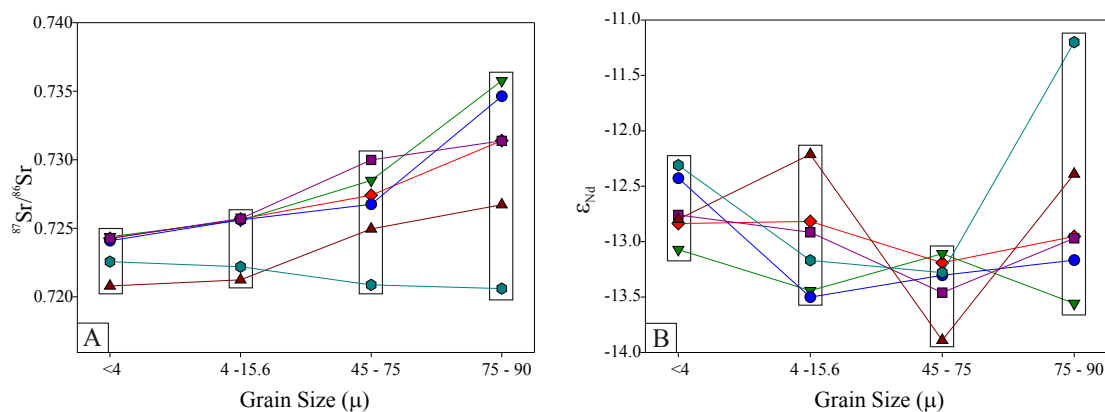


Fig. 4. (A) Variation of $^{87}\text{Sr}/^{86}\text{Sr}$ ratio in different grain size fractions (clay, silt, fine and coarse sand) of sediments from Nara river mouth and bet zones are shown. Also plotted are Sr-isotopic ranges of various probable sources. The different symbols represent six separate samples. (B) Variation of ϵ_{Nd} values in different grain size fractions of the same sediments mentioned above. The different symbols represent six separate samples.

Sr) in the source (e.g., muscovite; K-feldspar) break down to clays, finer fractions of sediments produced exhibit higher $^{87}\text{Sr}/^{86}\text{Sr}$ compared to that in coarser fractions (Garçon et al., 2014). Interestingly, however, we encountered significant amount of muscovite in coarser fractions of our samples, which prompted us for the above inference. In such a scenario, the $^{87}\text{Sr}/^{86}\text{Sr}$ of the clay fractions in our samples might not represent the composition of the sources, and therefore, the use of bulk sediment composition for provenance study would be the best bet.

4.3. Provenance of sediments and implications

The sediment load of the Indus in its upper reaches, north of its confluence with the rivers of Punjab (Fig. 1A), is dominated by material derived from sources in the Trans-Himalayas and its Sr-Nd isotopic compositions (IS: Indus at Skardu; Fig. 5A) are largely controlled by sediments derived from the ITSZ, Karakoram Batholith, and Ladakh Batholith (Clift et al., 2002). Predictably, sediments in the Indus delta and shelf (Fig. 5A) possess less radiogenic Nd (more radiogenic Sr) compared to that in sediments in the upper Indus, due to mixing with sediments from much older crustal rocks in the Higher Himalayan Crystalline (HHC) and Lesser Himalayas (LH), contributed through the rivers of Punjab (Clift et al., 2010). The sediments of the GRK having $^{87}\text{Sr}/^{86}\text{Sr}$ in the range of 0.7146–0.7307 and ϵ_{Nd} in the range of –14.3 to –11.4 although

overlap with the field for the Indus Delta (Fig. 5A), mostly possess more radiogenic Sr - a characteristic feature of the Lesser and Higher Himalayan sediments. The Luni and southern Thar (bordering the GRK basin) sediments have comparable ϵ_{Nd} and marginally higher $^{87}\text{Sr}/^{86}\text{Sr}$ values than those of the Indus sediments; however, possess more radiogenic Nd than the GRK sediments (Fig. 5A). These data clearly suggest that the GRK sediments neither represent any of the pure end-members such as the IS, the Luni, the Thar, the HHC, and the LH nor they are exclusively derived from the river Indus in its lower reaches or the Indus shelf. Since most of our samples are from the western GRK and that there was very limited (if any) sediment transport from the eastern GRK into the western GRK in the past (Glennie and Evans, 1976), the river Luni could not have been a major sediment source or pathway for the latter. Persistent ephemerality and aeolian activity from 8 ka onwards in the Luni basin (Kar et al., 2001), and dissimilar isotopic compositions of the Luni sediments with those of the western GRK sediments (Fig. 5A) also support this inference. A three component mixing model involving compositions of the IS, HHC and LH (Fig. 5A) reveals that although the GRK sediments deposited between 5.5 and 1.0 ka contain a large Trans-Himalayan component (up to 70%), there exists a significant component of the combined Higher and Lesser Himalayan rocks. The Trans-Himalayan component can easily be explained by the deposition of the Indus sediments (in lower reaches), directly or reworked, via the Thar desert,

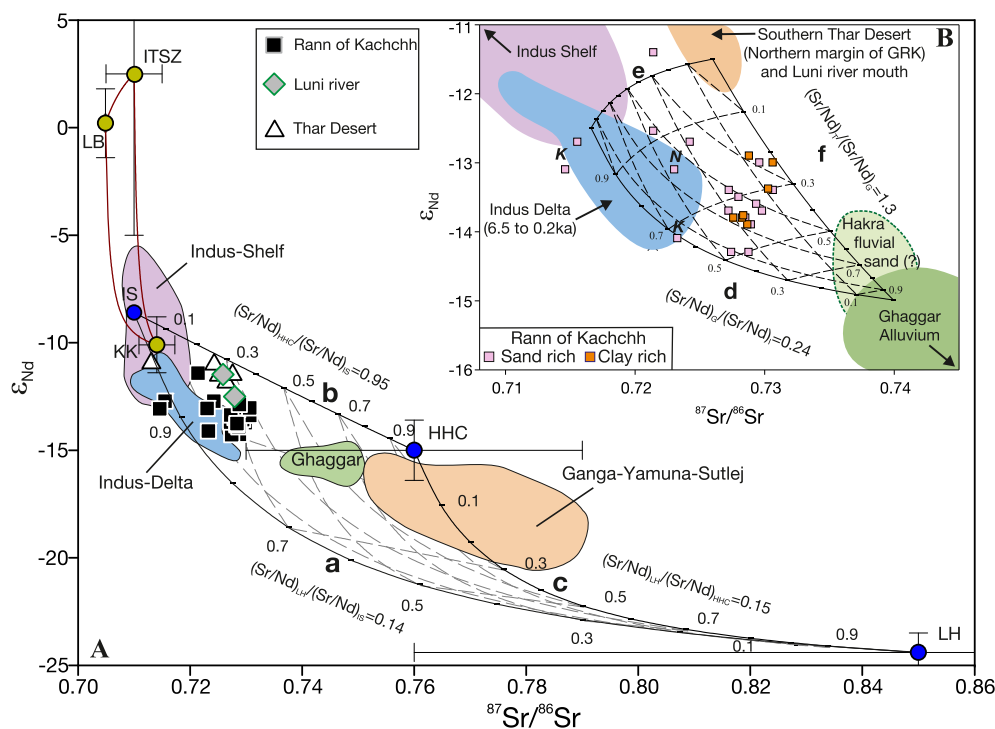


Fig. 5. (A) Plot of ϵ_{Nd} vs. $^{87}\text{Sr}/^{86}\text{Sr}$ for our samples compared with a ternary mixing grid. The three end-members are: (1) Indus sediments at Skardu (IS), (2) The Higher Himalayan Crystallines (HHC), and (3) The Lesser Himalayas (LH). IS component itself plots within another three component mixing grid involving the Indo-Tsangpo Suture Zone (ITSZ), Karakoram (KK) and Ladakh Batholith (LB) as end-members. Error bars cover the entire range of values for various components. Also shown are fields for sediments in the Indus Delta, present-day Ghaggar, and Ganga-Yamuna-Sutlej river systems. Curves a, b, and c represent binary mixing between typical compositions of two each of the end-members, whose compositions are: IS: Nd = 25 ppm; Sr = 210 ppm; $\epsilon_{\text{Nd}} = -8.6$; $^{87}\text{Sr}/^{86}\text{Sr} = 0.71$, HHC: Nd = 30 ppm; Sr = 240 ppm; $\epsilon_{\text{Nd}} = -15.0$; $^{87}\text{Sr}/^{86}\text{Sr} = 0.76$, and LH: Nd = 100 ppm; Sr = 120 ppm; $\epsilon_{\text{Nd}} = -24.4$; $^{87}\text{Sr}/^{86}\text{Sr} = 0.85$. Error bars of end-member compositions are at 3σ . **(B)** Plot of ϵ_{Nd} vs. $^{87}\text{Sr}/^{86}\text{Sr}$ for only the Great Rann of Kachchh samples, compared with a ternary mixing grid involving Indus river sediments, Thar Desert, and Ghaggar. Only ϵ_{Nd} values are available for fluvial sands of Hakra stream (East et al., 2015). However considering the fact that, Hakra is the downstream extension of Ghaggar, we have considered the range of $^{87}\text{Sr}/^{86}\text{Sr}$ values for Hakra sediments to be similar to Ghaggar. Hence, the zone defined for Hakra sediments in the figure are question marked. K and N represent samples from the Khadir Island and Nada Bet, respectively, in the eastern Great Rann of Kachchh (Fig. 1B). Curves d, e, and f represent binary mixing between typical compositions of two each of the end-members and these are: Indus Shelf/Delta: Nd = 30 ppm; Sr = 350 ppm; $\epsilon_{\text{Nd}} = -12.5$; $^{87}\text{Sr}/^{86}\text{Sr} = 0.7166$, southern Thar Desert: Nd = 40 ppm; Sr = 150 ppm; $\epsilon_{\text{Nd}} = -11.5$; $^{87}\text{Sr}/^{86}\text{Sr} = 0.726$, and Ghaggar: Nd = 100 ppm; Sr = 280 ppm; $\epsilon_{\text{Nd}} = -15$; $^{87}\text{Sr}/^{86}\text{Sr} = 0.740$. Data sources: present work and following references (Allègre and Othman, 1980; Clift et al., 2002; Najman, 2006; Schärer et al., 1990; Singh et al., 2016a; Tripathi et al., 2013).

and/or through storm tides entering into the western GRK through the Kori Creek that brings in silt and clay from the Indus delta with the help of long-shore currents. It should be noted that although the river Indus transports HHC-LH sediments contributed to it through its eastern tributaries, $^{87}\text{Sr}/^{86}\text{Sr}$ of the bulk sediments is lowered by a significant non-radiogenic Trans Himalayan component in the main channel - which is reflected in the isotopic composition of the Indus Delta (Clift et al., 2010). We, however, observe higher $^{87}\text{Sr}/^{86}\text{Sr}$ values ($>1.3\%$) in the sediments of western GRK (Fig. 5A), which suggest that there could have been other sources than the river Indus. Since in the present geomorphic set up direct deposition of the HHC-LH derived sediments into the basin is not possible, contribution from a third source is envisaged.

As mentioned earlier, the Ghaggar-Hakra channel originating from Siwaliks, made of rocks derived from the HHC-LH (Tripathi et al., 2013), could have been a pathway for the Himalayan contribution to the GRK basin, if it was connected to the river Nara in the past. Interestingly, the modern sediments of the Ghaggar, which should have had $^{87}\text{Sr}/^{86}\text{Sr}$ and ϵ_{Nd} in the range of that of the HHC/LH (Fig. 5A), possess lower $^{87}\text{Sr}/^{86}\text{Sr}$ and higher ϵ_{Nd} (Tripathi et al., 2013). This has been attributed to contributions from the Paleogene, sub-Himalayan foreland deposits of the Subathu Group (Tripathi et al., 2013). Assuming that the nature of various sediment sources has not changed since the mid-Holocene, we evaluated their contributions in the samples studied in this work (Fig. 5B). It is clear from the figure that the pre-modern sediments of the central and eastern GRK, from the Khadir Island (K) and Nada bet (N), although have Sr-Nd isotopic compositions similar to that of the Indus Delta (or Indus in lower reaches) are most likely derived from the river Luni, the Thar Desert and Mesozoic rocks exposed on the islands. In any case, the local sources do not produce significant amount of sediment and their compositions are very different from that of the western GRK sediments. Comparison of our isotopic data with model grids of a three component mixing, where sediments from the Ghaggar, southern Thar and the Indus delta/shelf are the end-members (Fig. 5B), suggests that 20–30% of the sediments deposited in the western GRK during 5.5 to 1.0 ka could have come through a now-defunct pathway connecting the Ghaggar, Hakra and Nara channels.

The samples that possess high radiogenic Sr (>0.728) are both sand and clay rich sediments, are not confined to any age bracket in the studied period, and a large number of them come from fluvially deposited horizons. If the finding of (Giosan et al., 2012) that there was fluvial activity in the Nara valley ~ 2.9 kyr ago were to be believed then our younger samples most likely represent monsoonal flooding events. Although the geochemical data for the GRK sediments clearly point towards a significant presence of sub-Himalayan (Siwalik) sediments that are not part of the Indus detritus, the overwhelming presence of the latter and southern Thar sand (up to 70%) makes it apparent that no perennial fluvial system was active in the Ghaggar-Hakra-Nara system during the Mature Harappan period. Our data nonetheless suggest that the Ghaggar-Hakra-Nara channels had remained active, possibly as a monsoon-fed system, until ~ 1.0 kyr ago. It was a sub-parallel system to the Indus, which transported sediments from the southern flanks of the Himalayas along with reworked aeolian sands into the GRK. Such an inference is not inconsistent with the inferences of (Giosan et al., 2012) and that these channels were active through intermittent flooding during the mid-Holocene, even after a substantial weakening of the monsoon post 4.2 ka (Enzel et al., 1999; Staubwasser et al., 2003; Wünnemann et al., 2010), before being covered by aeolian deposits. Although it is difficult to directly infer about the prevailing climatic conditions from our geochemical study, the sedimentological observations that substantial fluvial sand was deposited during 5.0–3.0 ka and 1.4–1.0 ka (Fig. 1B)

suggest enhanced rainfall, possibly caused by stronger Indian monsoon. Such an inference is supported by studies that propose short phases of monsoonal strengthening in peninsular India during 5100–4700 ka, 4105–2640 ka, and medieval warm period (Band et al., 2016; Banerji et al., 2016; Kotlia et al., 2015; Ngangom et al., 2016, 2012; Sarkar et al., 2000; Yadava and Ramesh, 2005) in the background of a regional decreasing trend since ~ 7 ka (Dixit et al., 2014; Sarkar et al., 2016).

5. Conclusions

Geochemistry and Sr-Nd isotopic data for mid-Holocene terrigenous detritus from the GRK reveal that the river Luni, Mesozoic rocks on the islands, and parabolic dune field of the south-eastern Thar are the primary contributors of sediments to the central and eastern GRK. On the other hand, sediments deposited in the western GRK during 5.5 to 1.0 kyr ago, although are primarily derived from the river Indus and transported into the basin by storm tides from the Indus delta and/or shelf; contain a significant amount of an independent sub-Himalayan component (20–30%). This sub-Himalayan component most likely was transported through the now defunct Ghaggar-Hakra-Nara river system. Since this river system, which ran parallel to the Indus, had dwindling water supply during the Harappan period, sediments carried by it must have reached the GRK only during heavy flooding events. Overwhelming presence of Indus detritus in the GRK makes it difficult to test the hypothesis of existence of a mega, glacial-fed river through the Ghaggar-Hakra-Nara channels during this period. These channels, however, were active until as late as 1.0 ka and therefore, their drying up may not have any causal relationship with the decline of the Harappan civilization.

Acknowledgments

We thank Navin Juyal for his encouragement, valuable suggestions and sharing of samples. Navin Juyal, P.S. Thakkar and A.D. Shukla participated in one of the field trips to the Great Rann of Kachchh. We also thank the two anonymous reviewers for their comments and suggestions. This work was supported by funding from the Department of Space, Government of India.

References

- Alizai, A., Carter, A., Clift, P.D., VanLaningham, S., Williams, J.C., Kumar, R., 2011a. Sediment provenance, reworking and transport processes in the Indus River by U–Pb dating of detrital zircon grains. *Glob. Planet. Change* 76, 33–55.
- Alizai, A., Clift, P.D., Giosan, L., VanLaningham, S., Hinton, R., Tabrez, A.R., Danish, M., 2011b. Pb isotopic variability in the modern–Pleistocene Indus River system measured by ion microprobe in detrital K-feldspar grains. *Geochim. Cosmochim. Acta* 75, 4771–4795. <http://dx.doi.org/10.1016/j.gca.2011.05.039>.
- Alizai, A., Clift, P.D., Still, J., 2016. Indus basin sediment provenance constrained using garnet geochemistry. *J. Asian Earth Sci.* 126, 29–57.
- Allègre, C.J., Othman, D. Ben, 1980. Nd–Sr isotopic relationship in granitoid rocks and continental crust development: a chemical approach to orogenesis. *Nature* 286, 335–342.
- Awasthi, N., Ray, J.S., Singh, A.K., Band, S.T., Rai, V.K., 2014. Provenance of the Late Quaternary sediments in the Andaman Sea: implications for monsoon variability and ocean circulation. *Geochim. Geophys. Geosyst.* 15, 3890–3906. <http://dx.doi.org/10.1002/2014GC005462>.
- Band, S., Yadava, M.G., Ramesh, R., Gupta, S., Polyak, V.J., Asmerom, Y., 2016. Holocene Monsoon variability using stalagmite record from Dandak cave, India. In: *Goldschmidt Conference Abstracts*, vol. 2016, p. 152.
- Banerji, U.S., Bhushan, R., Jull, A.J.T., 2016. Mid–late Holocene monsoonal records from the partially active mudflat of Diu Island, southern Saurashtra, Gujarat, western India. *Quat. Int.* <http://dx.doi.org/10.1016/j.quaint.2016.09.060>.
- Biswas, S.K., 1987. Regional tectonics framework, structure and evolution of the western marginal basins of India. *Tectonophysics* 135, 307–327.
- Clift, P.D., Carter, A., Giosan, L., Durcan, J., Duller, G. a. T., Macklin, M.G., Alizai, A., Tabrez, A. R., Danish, M., VanLaningham, S., Fuller, D.Q., 2012. U–Pb zircon dating evidence for a pleistocene sarasvati river and capture of the Yamuna river. *Geology* 40, 211–214. <http://dx.doi.org/10.1130/G32840.1>.

- Clift, P.D., Giosan, L., Blusztajn, J., Campbell, I.H., Allen, C., Pringle, M., Tabrez, A.R., Danish, M., Rabbani, M.M., Alizai, A., Carter, A., Lückge, A., 2008. Holocene erosion of the Lesser Himalaya triggered by intensified summer monsoon. *Geology* 36, 79–82. <http://dx.doi.org/10.1130/G24315A.1>.
- Clift, P.D., Giosan, L., Carter, A., Garzanti, E., Galy, V., Tabrez, A.R., Pringle, M., Campbell, I.H., France-Lanord, C., Blusztajn, J., Allen, C., Alizai, A., Luckge, A., Danish, M., Rabbani, M.M., 2010. Monsoon control over erosion patterns in the Western Himalaya: possible feed-back into the tectonic evolution. In: Clift, P.D., Tada, R., Zheng, H. (Eds.), *Monsoon Evolution and Tectonics - Climate Linkage in Asia*. The Geological Society of London, pp. 185–218. <http://dx.doi.org/10.1144/SP342.12>.
- Clift, P.D., Lee, J.I., Hildebrand, P., Shimizu, N., Layne, G.D., Blusztajn, J., Blum, J.D., Garzanti, E., Ali, A., 2002. Nd and Pb isotope variability in the Indus River System: implications for sediment provenance and crustal heterogeneity in the Western Himalaya. *Earth Planet. Sci. Lett.* 200, 91–106.
- Dixit, Y., Hodell, D.A., Sinha, R., Petrie, C.A., 2014. Abrupt weakening of the Indian summer monsoon at 8.2 kyrBP. *Earth Planet. Sci. Lett.* 391, 16–23. <http://dx.doi.org/10.1016/j.epsl.2014.01.026>.
- East, A.E., Clift, P.D., Carter, A., Alizai, A., VanLaningham, S., 2015. Fluvial – eolian interactions in Sediment routing and sedimentary signal buffering: an example from the Indus basin and Thar Desert. *J. Sediment. Res.* 85, 715–728. <http://dx.doi.org/10.2110/jsr.2015.42>.
- Enzel, Y., Ely, L.L., Mishra, S., Ramesh, R., Amit, R., Lazar, B., Rajaguru, S.N., Baker, V.R., Sandler, A., 1999. High-Resolution Holocene environmental changes in the thar desert, northwestern India. *Sci. (80-.)* 284, 125–128.
- Garçon, M., Chauvel, C., France-lanord, C., Limonta, M., Garzanti, E., 2014. Which minerals control the Nd – Hf – Sr – Pb isotopic compositions of river sediments. *Chem. Geol.* 364, 42–55. <http://dx.doi.org/10.1016/j.chemgeo.2013.11.018>.
- Garzanti, E., Vezzoli, G., Andò, S., Paparella, P., Clift, P.D., 2005. Petrology of Indus river sands: a key to interpret erosion history of the western himalayan syntaxis. *Earth Planet. Sci. Lett.* 229, 287–302. <http://dx.doi.org/10.1016/j.epsl.2004.11.008>.
- Gaur, A.S., Vora, K.H., Murali, R.M., Jayakumar, S., 2013. Was the Rann of Kachchh navigable during the harappan times (mid-holocene)? An archaeological perspective. *Curr. Sci.* 105, 1485–1491.
- Ghose, B., Kar, A., Husain, Z., 1979. The lost courses of the Saraswati river In the great indian desert: new evidence from landsat imagery. *Geogr. J.* 145, 446–451.
- Giosan, L., Clift, P.D., Macklin, M.G., Fuller, D.Q., Constantinescu, S., Durcan, J. A., Stevens, T., Duller, G. a T., Tabrez, A.R., Gangal, K., Adhikari, R., Alizai, A., Filip, J., VanLaningham, S., Syvitski, J.P.M., 2012. Fluvial landscapes of the Harappan civilization. *Proc. Natl. Acad. Sci. U. S. A.* 109, E1688–E1694. <http://dx.doi.org/10.1073/pnas.1112743109>.
- Glennie, K.W., Evans, G., 1976. A reconnaissance of the recent sediments of the ranns of Kutch, India. *Sedimentology* 23, 625–647.
- Goldstein, S.J., Jacobsen, S.B., 1988. Nd and Sr isotopic systematics of river water suspended material: implications for crustal evolution. *Earth Planet. Sci. Lett.* 87, 249–265.
- Gupta, A.K., Sharma, J.R., Sreenivasan, G., 2011. Using satellite imagery to reveal the course of an extinct river below the Thar Desert in the Indo-Pak region. *Int. J. Remote Sens.* 32, 5197–5216.
- Kar, A., Singhvi, A.K., Rajaguru, S.N., Juyal, N., Thomas, J.V., Banerjee, D., Dhir, R.P., 2001. Reconstruction of the late quaternary environment of the lower Luni plains, thar desert, India. *J. Quat. Sci.* 16, 61–68.
- Kenoyer, J.M., 2008. Indus civilization. In: *Encyclopedia of Archaeology*. Elsevier, New York, pp. 715–733.
- Khonde, N.N., Maurya, D.M., Chamyal, L.S., 2016. Late Pleistocene-Holocene clay mineral record from the Great Rann of Kachchh basin, Western India: implications for palaeoenvironments and sediment sources. *Quat. Int.* 1–13. <http://dx.doi.org/10.1016/j.quaint.2016.07.024>.
- Kochar, R., 2000. *Vedic People: Their History and Geography*. Orient Longman, Hyderabad.
- Kotlia, B.S., Singh, A.K., Joshi, L.M., Dhaila, B.S., 2015. Precipitation variability in the indian central Himalaya during last ca. 4,000 years inferred from a speleothem record: impact of indian summer monsoon (ISM) and Westerlies. *Quat. Int.* 371, 244–253. <http://dx.doi.org/10.1016/j.quaint.2014.10.066>.
- Limmer, D.R., Böning, P., Giosan, L., Ponton, C., Köhler, C.M., Cooper, M.J., Tabrez, A.R., Clift, P.D., 2012. Geochemical record of Holocene to recent sedimentation on the western Indus continental shelf, Arabian sea. *Geochem. Geophys. Geosyst.* 13 <http://dx.doi.org/10.1029/2011GC003845>.
- Malik, J.N., Merh, S.S., Sridhar, V., 1999. Palaeo-delta complex of Vedic Saraswati and other ancient rivers of north-western India. *Mem. Geol. Soc. India* 42, 163–174.
- Mathew, G., Singhvi, A.K., Karanth, V., 2006. Luminescence chronometry and geomorphic evidence of active fold growth along the Kachchh Mainland Fault (KMF), Kachchh, India: seismotectonic implications. *Tectonophysics* 422, 71–87.
- Maurya, D.M., Khonde, N., Das, A., Chowksey, V., Chamyal, L.S., 2013. Subsurface sediment characteristics of the Great Rann of Kachchh, western India based on preliminary evaluation of textural analysis of two continuous sediment cores. *Curr. Sci.* 104, 859–862.
- Maurya, D.M., Thakkar, M.G., Chamyal, L.S., 2003. Quaternary geology of the arid zone of Kachchh: terra Incognita. *Proc. Indian Natl. Sci. Acad.* 69A, 123–135.
- Maurya, D.M., Thakkar, M.G., Patidar, A.K., Bhandari, S., Goyal, B., Chamyal, L.S., 2008. Late Quaternary geomorphic evolution of the coastal zone of Kachchh, Western India. *J. Coast. Res.* 24, 746–758.
- Merh, S.S., 2005. The great Rann of Kachchh: perceptions of a field geologist. *J. Geol. Soc. India* 65, 9–25.
- Meyer, I., Davies, G.R., Stuut, J.-B.W., 2011. Grain size control on Sr-Nd isotope provenance studies and impact on paleoclimate reconstructions: an example from deep-sea sediments offshore NW Africa. *Geochem. Geophys. Geosyst.* 12 <http://dx.doi.org/10.1029/2010GC003355>.
- Misra, V.N., 1984. Climate: a factor in the rise and fall of Indus Civilization. In: *Frontiers of the Indus Civilization*. Books and Books, New Delhi, pp. 469–489.
- Mughal, M.R., 1997. *Ancient Cholistan: Archaeology and Architecture*. Ferozsons, Lahore, Pakistan.
- Murray, A.S., Wintle, A.G., 2000. Luminescence dating of quartz using an improved single-aliquot regenerative-dose protocol. *Radiat. Meas.* 32, 57–73.
- Najman, Y., 2006. The detrital record of orogenesis: a review of approaches and techniques used in the Himalayan sedimentary basins. *Earth-Sci. Rev.* 74, 1–72. <http://dx.doi.org/10.1016/j.earscirev.2005.04.004>.
- Ngangom, M., Bhandari, S., Thakkar, M.G., Shukla, A.D., Juyal, N., 2016. Mid-Holocene extreme hydrological events in the eastern Great Rann of Kachchh, western India. *Quat. Int.* <http://dx.doi.org/10.1016/j.quaint.2016.10.017>.
- Ngangom, M., Thakkar, M.G., Bhushan, R., Juyal, N., 2012. Continental – marine interaction in the vicinity of the Nara river during the last 1400 years, great Rann of. *Curr. Sci.* 103, 1339–1342.
- Oldham, C.F., 1893. The Saraswati and the lost river of the Indian desert. *J. R. Asiat. Soc.* 34, 49–76.
- Oldham, R.D., 1926. The Cutch (Kachh) earthquake of 16th June 1819 with a rivision of the great earthquake of 12th June 1897. *Mem. Geol. Surv. India* 46, 71–147.
- Pal, Y., Sahai, B., Sood, R.K., Agarwal, D.P., 1980. Remote sensing of the “lost” Saraswati river. *Proc. Indian Natl. Sci. Acad. (Earth Planetary Sci.)* 89, 317–331.
- Possehl, G.L., 2002. The Indus Civilization: a Contemporary Perspective. AltaMira Press, Lanham, Maryland.
- Raczek, I., Jochum, K.P., Hofmann, A.W., 2001. Neodymium and strontium isotope data for USGS reference GSP-1, GSP-2 and eight MPI-DING reference glasses. *Geostand. Newsl.* 27, 173–179.
- Radhakrishnan, B.P., Merh, S.S., 1999. Vedic sarasvati: evolutionary history of a lost river of northwestern India. *Mem. Geol. Soc. India* 42, 5–13.
- Rajendran, C.P., Ranjendran, K., 2001. Characteristics of deformation and past seismicity Associated with the 1819 Kutch earthquake, northwestern India. *Bull. Seismol. Soc. Am.* 91, 407–426.
- Sarkar, A., Mukherjee, A.D., Bera, M.K., Das, B., Juyal, N., Morthekai, P., Deshpande, R.D., Shinde, V.S., Rao, L.S., 2016. Oxygen isotope in archaeological bioapatites from India: implications to climate change and decline of Bronze Age Harappan civilization. *Sci. Rep.* 6, 26555. <http://dx.doi.org/10.1038/srep26555>.
- Sarkar, A., Ramesh, R., Somayajulu, B.L.K., Agnihotri, R., Jull, A.J.T., Burr, O.S., 2000. High resolution Holocene monsoon record from the eastern Arabian Sea. *Earth Planet. Sci. Lett.* 177, 209–218. [http://dx.doi.org/10.1016/S0012-821X\(00\)00053-4](http://dx.doi.org/10.1016/S0012-821X(00)00053-4).
- Scharer, U., Copeland, P., Harrison, T.M., Searle, M.P., 1990. Age, cooling history and origin of post-collisional leucogranite in the Karakoram batholith: a multi-system isotope study. *J. Geol.* 98, 233–251.
- Singh, A., Paul, D., Sinha, R., Thomsen, K.J., Gupta, S., 2016a. Geochemistry of buried river sediments from Ghaggar Plains, NW India: multi-proxy records of variations in provenance, paleoclimate, and paleovegetation patterns in the Late Quaternary. *Paleogeogr. Paleoclimatol., Paleoecol.* 449, 85–100. <http://dx.doi.org/10.1016/j.palaeo.2016.02.012>.
- Singh, A., Paul, D., Sinha, R., Thomsen, K.J., Gupta, S., 2016b. Reply to the comment on “Geochemistry of buried river sediments from Ghaggar Plains, NW India: multi-proxy records of variations in provenance, paleoclimate, and paleovegetation patterns in the late quaternary” by Singh et al. (2016). *Paleogeogr. Pal. Paleogeogr. Paleoclimatol. Paleoecol.* 455, 68–70. <http://dx.doi.org/10.1016/j.palaeo.2016.05.001>.
- Singh, S.K., Rai, S.K., Krishnaswami, S., 2008. Sr and Nd isotopes in river sediments from the Ganga Basin: sediment provenance and spatial variability in physical erosion. *J. Geophys. Res.* 113 <http://dx.doi.org/10.1029/2007JF000909>.
- Singhvi, A.K., Kar, A., 2004. The aeolian sedimentation record of the Thar desert. *Proc. Indian Acad. Sci. (Earth Planetary Sci.)* 113, 371–401.
- Sinha, R., Yadav, G.S., Gupta, S., Singh, A., Lahiri, S.K., 2013. Geo-electric resistivity evidence for subsurface palaeochannel systems adjacent to Harappan sites in northwest India. *Quat. Int.* 308–309, 66–75. <http://dx.doi.org/10.1016/j.quaint.2012.08.002>.
- Staubwasser, M., Sirocko, F., Grootes, P.M., Segl, M., 2003. Climate change at the 4.2 ka BP termination of the Indus valley civilization and Holocene south Asian monsoon variability. *Geophys. Res. Lett.* 30, 1425. <http://dx.doi.org/10.1029/2002GL016822>.
- Syvitski, J.P.M., Kettner, A.J., Overeem, I., Giosan, L., Brakenridge, G.R., Hannon, M., Bilham, R., 2013. Anthropocene metamorphosis of the Indus Delta and lower floodplain. *Anthropocene* 3, 24–35. <http://dx.doi.org/10.1016/j.ancene.2014.02.003>.
- Tanaka, T., Togashi, S., Kamioka, H., Amakawa, H., 2000. JNdi-1: a neodymium isotopic reference in consistency with LaJolla neodymium. *Chem. Geol.* 168, 279–281.
- Tripathi, J.K., Bock, B., Rajamani, V., 2013. Nd and Sr isotope characteristics of Quaternary Indo-Gangetic plain sediments: source distinctiveness in different geographic regions and its geological significance. *Chem. Geol.* 344, 12–22. <http://dx.doi.org/10.1016/j.chemgeo.2013.02.016>.
- Tyagi, A.K., Shukla, A.D., Bhushan, R., Thakkar, P.S., Thakkar, M.G., Juyal, N., 2012.

- Mid-Holocene sedimentation and landscape evolution in the western Great Rann of Kachchh, India. *Geomorphology* 151, 89–98. <http://dx.doi.org/10.1016/j.geomorph.2012.01.018>.
- Valdiya, K.S., 2013. The river Saraswati was a Himalayan-born river. *Curr. Sci.* 104, 42–54.
- Wright, R.P., Bryson, R.A., Schuldenrein, J., 2008. Water supply and history: Harappa and the Beas regional survey. *Antiquity* 82, 37–48.
- Wünnemann, B., Damske, D., Tarasov, P., Kotliar, B.S., Reinhardt, C., Bloemendal, J., Diekmann, B., Hartmann, K., Krois, J., Riedel, F., Arya, N., 2010. Hydrological evolution during the last 15 kyr in the Tso Kar lake basin (Ladakh, India), derived from geomorphological, sedimentological and palynological records. *Quat. Sci. Rev.* 29, 1138–1155. <http://dx.doi.org/10.1016/j.quascirev.2010.02.017>.
- Yadava, M.G., Ramesh, R., 2005. Monsoon reconstruction from radiocarbon dated tropical Indian speleothems. *Holocene* 15, 48–59. <http://dx.doi.org/10.1191/0959683605h1783rp>.
- Yadava, M.G., Ramesh, R., 1999. Speleothems - useful proxies for past monsoon rainfall. *J. Sci. Ind. Res.* 58, 339–348.